European Journal of Neuroscience, Vol. 20, pp. 2483–2488, 2004

SHORT COMMUNICATION
When 'go' and 'nogo' are equally frequent: ERP components and cortical tomography

Aureliu Lavric,[1] Diego A. Pizzagalli[2] and Simon Forstmeier[3]
[1]School of Psychology, University of Exeter, Washington Singer Laboratories, Perry Road, Exeter EX4 4QG, England
[2]Department of Psychology, Harvard University, 1220 William James Hall, 33 Kirkland Street Cambridge, MA 02138, USA
[3]Center for Psychobiological and Psychosomatic Research, University of Trier, St. Franziska-Stift, Franziska-Puricelli-Strasse 3, 55543 Bad Kreuznach, Germany

Keywords: conflict, event-related potentials, go–nogo, inhibition, localization, N2

Abstract

In human electrophysiology, a considerable corpus of studies using event-related potentials have investigated inhibitory processes by employing the 'go–nogo' paradigm, which requires responding to one type of event while withholding the response to another type of event. Two event-related potential waveform features (N2 and P3) have been associated with larger amplitude in *nogo* trials than in *go* trials. Traditionally, these differences were thought to reflect response inhibition. Recently, the source localization of N2 to the anterior cingulate cortex, as well as the colocalization of N2 with error-related negativity, has been interpreted in terms of conflict monitoring. In order to isolate the contribution of inhibitory processes, we matched the frequency of the *go* and *nogo* events, thus minimizing differences in response conflict between event types. A data-driven analytical procedure contrasted *go* with *nogo* events across the entire event-related potential segment and found that N2 reliably differentiated between the two conditions while P3 did not. Tomographical analyses of the N2 difference observed in conditions of equal *go* and *nogo* trial frequency localized N2 to the right ventral and dorsolateral prefrontal cortex. Because a growing body of evidence implicates these brain regions in inhibitory processes, we conclude that N2 does, at least in part, reflect inhibition.

Introduction

An enduring question in cognitive neuroscience is how the cognitive system resolves the competition between conflicting behavioural tendencies. This problem has prompted the use of the 'go–nogo' experimental paradigm, in conjunction with event-related potentials (ERP), which are electroencephalographic (EEG) changes time-locked to sensory, motor, or cognitive events. Typically, a 'go–nogo' design requires subjects to generate an overt or covert response (e.g. press a key or count) to one event type (*go*), usually frequent, and to withhold the response to another type of event (*nogo*), usually rare (Pfefferbaum *et al*., 1985).

Two features of the ERP waveform have been reliably associated with the go–nogo manipulation: (i) an enhanced positive peak at anterior electrodes in *nogo* relative to *go* ERPs in the 300–500 ms range poststimulus onset, referred to as P3 (Roberts *et al*., 1994) and (ii) a larger negative shift (N2) relative to *go* stimuli, with a central-anterior scalp distribution (e.g. Jodo & Kayama, 1992; Eimer, 1993). Traditionally, N2 and P3 amplitude differences have been assumed to reflect the inhibition of the prepotent response in *nogo* trials (N2 and P3 latency effects have also been found, see Roche *et al*., in press).

Recently, it has been proposed that N2 reflects conflict monitoring, rather than inhibition (Nieuwenhuis *et al*., 2003). This account is based principally on the location of the dipole-modelled source of N2 in the anterior cingulate cortex (ACC). It is also motivated by the colocalization of the N2 generator with that of the error-related negativity to ACC (Van Veen & Carter, 2002; Nieuwenhuis *et al*., 2003; though for an alternative perspective on the relationship between N2 and the error-related negativity, see Falkenstein *et al*., 1999). Indeed, evidence from a range of neuroimaging paradigms suggests that ACC monitors conflict between response tendencies (Braver *et al*., 2001). In contrast, the traditional inhibition account of the N2 go–nogo effect would predict a more inferior/lateral cortical substrate for N2: neuroimaging studies in humans and neurophysiological work in nonhuman primates point to the role of the ventral prefrontal cortex (vPFC) and dorsolateral prefrontal cortex (dLPFC), in response inhibition (Watanabe, 1986; Konishi *et al*., 1999; Morita *et al*., 2004). Interestingly, in a recent ERP localization study, Bokura *et al*. (2001) found both ACC and vPFC loci of N2, thus suggesting that the two systems, involved in conflict-monitoring (ACC) and inhibition (vPFC, dLPFC), may both contribute to the observed N2 effect.

Trial type frequency is a critical variable that has been largely overlooked in ERP go–nogo investigations. All but very few studies contrasted frequent *go* events with rare *nogo* events. Consequently, at least some of the observed ERP differences between *go* and *nogo* stimuli could be due to frequency ('relative novelty'), rather than other processes (e.g. inhibition). P3, in particular, is known to be very sensitive to stimulus frequency (Yamaguchi & Knight, 1991). In the context of a potentially dual anatomical substrate of the N2 effect, one can attempt to isolate the contribution of the inhibitory component. If trial types are matched for frequency, and, presumably, for the degree of response conflict, an enhanced N2 in *nogo* trials would reflect inhibition. An enhanced *nogo* N2 was indeed found in studies that matched trial type frequency (e.g. Jodo & Kayama, 1992; Nieuwenhuis *et al*., 2003). The question still awaiting an answer is

Correspondence: Dr Aureliu Lavric, as above.
E-mail: A.Lavric@exeter.ac.uk

Received 12 May 2004, revised 28 July 2004, accepted 3 August 2004

doi:10.1111/j.1460-9568.2004.03683.x

whether the elimination of the distributional discrepancy between *go* and *nogo* events will enhance the contribution of the ventral and/or lateral frontal brain regions to the observed N2 scalp effect.

To directly address this issue a between-subjects design that contrasted rare *go* responses with rare *nogo* responses to the same physical stimuli was implemented. An analytical procedure tested *go* vs. *nogo* differences time-point by time-point across the entire ERP segment, circumventing the problem of limiting the analysis to any particular component(s). N2 localization hypotheses were tested using tomographic analyses. We hypothesized that, by matching the *go* and *nogo* conditions for stimulus frequency and amount of conflict generated, while preserving prepotent responses, N2 effects in the present study would primarily reflect inhibitory processes subserved by vPFC and dLPFC regions.

Method

Subjects

Thirty right-handed participants (14 females; mean ± SD age 20.03 ± 2.11 years, range 18–27 years) volunteered to participate in the study; the recruitment was done on the university campus via posters. The procedure was approved by the departmental ethics committee (Department of Psychology, University of Warwick, UK), it conformed to the Code of Ethics of the World Medical Association (Declaration of Helsinki). All subjects provided informed written consent.

Apparatus

Stimuli were displayed using an IBM compatible PC and the programming language for stimulus presentation EXPE 6 (Pallier *et al*., 1997). A NeuroSciences Imager Series 3 (Warwick, UK) system and a 32-tin-electrode elastic cap (ElectroCap International Inc., Eaton, Ohio, USA) were used for EEG data-collection.

Go–nogo task and procedure

The instruction was to discriminate between two kinds of geometrical shapes: rectangles and nonrectangles, presented in white against a black background in the centre of the screen with a probability of 0.75 and 0.25 (i.e. nonrectangles were rare; they included rombuses, elipses and circles, which were equiprobable). Shapes were 1.2° of visual angle, as determined by the distance from the centre of the shape to the most distant point from the centre. Participants were divided in two groups of equal size and gender distribution. Group 1 had to press a key whenever they saw a nonrectangle and ignore the rectangles (the rare *go* condition); group 2 to had to press a key for rectangles and ignore the nonrectangles (the rare *nogo* condition). The structure of a 3600-ms trial was the following: fixation cross (500 ms), blank screen (500 ms), geometrical shape (300 ms), blank screen (1000 ms), feedback screen ('…' when the instructions were correctly executed, or 'Error', or 'No response'; 1000 ms), blank screen (300 ms). The response deadline (for *go* events) was 1300 ms. The task was administered in blocks of 124 trials. All subjects performed one practice block and two test blocks (248 test trials); total session duration, including preparation for recording, was ∼1 h.

Electrophysiological recording and data preprocessing

EEG epochs of 2124 ms (100 ms prestimulus and 2024 ms poststimulus) were recorded for rare events (nonrectangles), with a 0.1–40 Hz bandpass, a 333 Hz sampling rate, linked earlobes as reference and AFz as ground. Two channels were used for the horizontal EOG (at the outer canthi of both eyes) and two for recording the vertical EOG (supra- and suborbitally at the right eye). Scalp channels (28) included all sites of the10–20 convention and the following sites from the extended 10–20 convention: FC5, FC6, CP1, CP2, CP5, CP6, PO1, PO2, Oz. ERP segments, 768 ms long (plus 100 ms baseline), time-locked to the presentation of nonrectangles were obtained for each subject. From the total of 62 segments (248 test trials × probability of 0.25), only those associated with the correct behavioural response were kept. Subsequently, an automated procedure excluded all segments that contained amplitudes ± 100 μV in any channel. Finally, all segments were visually inspected and those containing eye-movement, amplifier or muscle artefact were discarded. All subjects had at least 30 artifact-free trials; the two experimental groups did not diverge in the number of artefact-free trials (*go* mean ± SD, 45.13 ± 5.85; *nogo*, 44.73 ± 5.77; $t_{28} = 0.18$, $P > 0.5$).

ERP analysis

Topographic analysis of variance (TANOVA, Pascual-Marqui *et al*., 1995; http://www.unizh.ch/keyinst/NewLORETA/LORETA01.htm) was employed for comparisons between the ERPs to nonrectangles in the *go* and *nogo* conditions. This procedure computes the overall dissimilarity between ERP scalp topographies, conceptualized as vectors defined by *n* scalp electrodes ($n = 28$ here). We used TANOVA and independent samples *t*-tests to compute the dissimilarity at each of the 256 time-points of the ERP, while performing random permutations (1000) to correct for false positives (Nichols & Holmes, 2002). Prior to being submitted to TANOVA, the average ERP segments of all participants were average-referenced and transformed to a global field power of 1. The latter ensures that the dissimilarity is not influenced by higher activity across the scalp in one of the conditions (experimental groups).

Subject to reliable TANOVA differences between conditions in the N2–P3 range, temporal Principal Components Analysis (PCA, Donchin & Heffley, 1978) was employed to ensure that the observed difference (e.g. N2) was not due to temporally overlapping components (e.g. P2 or P3). Time-points (256) were used as variables and electrodes × participants ($28 \times 30 = 840$) as observations in a varimax-rotated PCA performed on the covariance matrix, with the eigenvalue = 1 set as a component identification criterion. Only components that explained over 2% variance were considered. Statistical analysis (ANOVA) was performed on the factor scores of the PCA component temporally closest to the ERP effect of interest.

To facilitate direct comparisons with other ERP go–nogo studies, a traditional amplitude analysis (ANOVA and *t*-tests) on the mean ERP amplitude within TANOVA-defined time-windows was also performed. All ANOVAs had three factors: Condition (*go* vs. *nogo*), Scalp region (anterior frontal – FP1,FP2,F3,F4,F7,F8; posterior frontal – C3,C4,FC5,FC6; temporal – T7,T8,P7,P8; parietal – CP1,CP2,CP5,CP6,P3,P4; parietal-occipital – PO1,PO2,O1,O2) and Hemisphere (left vs. right). The Greenhouse-Geisser procedure was used to correct for sphericity violations, where necessary, and scalp region *t*-tests were Bonferroni-corrected.

Cortical localization

Subject to reliable TANOVA differences between conditions in the N2–P3 range, Low-Resolution Electromagnetic Tomography (LORETA, Pascual-Marqui *et al*., 1994; Pascual-Marqui, 1999; http://www.

unizh.ch/keyinst/NewLORETA/LORETA01.htm) was used for computing the 3-D intracerebral distribution of current density. The algorithm solves the inverse problem by assuming related strengths and orientations of sources, which mathematically corresponds to finding the smoothest activity distribution (no assumption is made about the number of sources). LORETA computes, at each voxel, current density as the linearly weighted sum of the scalp electric potentials. The voxel resolution of the method is 7 mm and the solution space consists of 2394 voxels, restricted to cortical grey matter and hippocampi. The version used in the present study (Pasqual-Marqui, 1999) was registered to the MNI305 brain atlas. To provide Brodmann's area and region label for a specific MNI coordinate, LORETA first determines the nearest grey matter voxel using a lookup table created via the Talairach Daemon (Lancaster *et al*., 2000), and then estimates a conversion from MNI space to Talairach space (Talairach & Tournoux, 1988) using the transform by Bret (Brett *et al*., 2002; http://www.mrc-cbu.cam.ac.uk/Imaging/Common/mnispace.shtml). Of note, recent studies comparing LORETA-based EEG data with traditional tomographic techniques, including PET (Pizzagalli *et al*., 2004) and fMRI (Mulert *et al*., 2004) have reported important cross-modal validity for the LORETA algorithm.

LORETA solutions were: (i) obtained for each time point in the time window(s) of TANOVA differences from average-referenced ERPs; (ii) averaged within the time window of interest; (iii) normalized within-subjects, by dividing current density at each voxel by the average activity of all voxels; (iv) log-transformed (the latter two steps are standard for LORETA independent samples comparisons); (v) submitted to voxel-wise *t*-tests, corrected for multiple comparisons (Nichols & Holmes, 2002).

Results

Behavioural results

The difference in the relative *go*/nogo trial frequency resulted in a larger proportion of misses in the *go* (rare *go*) group than in the *nogo* (rare *nogo*) group (mean percentage ± SD: *go*, 12.58 ± 3.35%; *nogo*, 2.04 ± 1.77%; $t_{28} = 10.77$, $P < 0.000$), and more false alarms in the *nogo* relative to the *go* group (*go*, 1.18 ± 0.71%; *nogo*, 14.19 ± 4.36%; $t_{28} = -11.40$, $P < 0.000$). Responses were reliably faster in the *nogo* condition (*go*, 547 ± 78 ms; *nogo*, 470 ± 75 ms; $t_{28} = -2.72$, $P < 0.05$). The proportion of misses in the *go* group was similar to the proportion of false alarms in the *nogo* (12.58% and 14.19%, respectively).

ERPs

TANOVA identified two time-windows, each ~20–25 ms long, in which all time-points were associated with significant differences between scalp vectors (topographies): 133–157 ms and 235–256 ms after stimulus onset. The two differences correspond temporally to the ERP peaks N1 and N2, in which the *nogo* ERPs had a more negative amplitude than the *go* ERPs (see Fig. 1a). No other time-points in the ERP waveform were associated with reliable scalp topography differences. In the P3 range (350–450 ms after stimulus onset), at no time-point scalp differences approached significance (lowest $P = 0.32$).

On the basis of visual inspection, it may appear that the N2 difference is an augmentation of an earlier difference in the P2 peak (190–215 ms). In order to confidently ascertain that the observed N2 difference is not a consequence of other ERP components in the temporal vicinity (e.g. P2), ANOVA was performed on the PCA component that was closest to the middle of the TANOVA N2 (235–256 ms) difference window- the PCA component that peaked at 262 ms (see Fig. 1B). ANOVA revealed a significant main effect of Condition ($F_{1,28} = 19.26$, $P < 0.001$) and Condition-by-Region interaction ($F_{4,112} = 5.17$, $P < 0.05$), with pairwise comparisons significant in the following scalp regions: frontal anterior, left and right ($t_{28} = 4.61$, $P < 0.01$; $t_{28} = 4.82$, $P < 0.01$, respectively); frontal posterior, left and right ($t_{28} = 4.38$, $P < 0.01$; $t_{28} = 3.52$, $P < 0.05$, respectively); and parietal, left and right ($t_{28} = 4.03$, $P < 0.01$; $t_{28} = 3.28$, $P < 0.05$, respectively). ANOVA was also performed on the earlier PCA component that temporally overlaps the P2 component of the ERP: no reliable main effect of Condition ($F_{1,28} = 0.10$ (ns) or Condition-by-Region interaction ($F_{1,28} = 1.43$ (ns) was found.

To facilitate comparisons with other ERP go–nogo studies, ANOVA was run on the amplitude averaged within the TANOVA defined window (235–256 ms). It revealed a reliable main effect of Condition ($F_{1,28} = 12.37$, $P < 0.005$) and Condition-by-Region interaction ($F_{4,112} = 3.75$, $P < 0.05$). Independent sample *t*-tests for scalp regions (10 tests: 5 regions*2 hemispheres) were significant in the frontal anterior region, left and right ($t_{28} = 3.54$, $P < 0.05$; $t_{28} = 3.77$, $P < 0.05$, respectively), frontal posterior region, left and right ($t_{28} = 3.16$, $P < 0.05$; $t_{28} = 3.39$, $P < 0.05$, respectively) and parietal region, left and right ($t_{28} = 3.10$, $P < 0.05$; $t_{28} = 3.29$, $P < 0.05$, respectively).

Cortical localization

LORETA analyses were performed on the N2 difference in the TANOVA-identified window (235–256 ms). Tests on the whole solution space identified a small vPFC region in the right hemisphere, associated with more activation (higher current density) in the *nogo* condition (see Fig. 1C). No other differences were found. In order to test specific hypotheses regarding localization of go–nogo effects (see Introduction), in addition to LORETA tests run on the entire solution space (2394 voxels), voxel-by-voxel tests were also performed on the same time-window (235–256 ms) in 3 regions of interest (ROIs): anterior cingulate (Brodmann's areas 24, 25 and 32), ventral prefrontal (Brodmann's areas 11 and 47) and dorsolateral prefrontal (Brodmann's areas 10 and 46). Each ROI included all LORETA voxels in the respective Brodmann's areas: vPFC-130, ACC-174, dLPFC-196. ROI tests found reliable effects predominantly in the vPFC ROI: 32 voxels (10.98 cm^3) were more active in the *nogo* condition; some differences (1 voxel) were also discovered in dLPFC (see Fig. 1D). No voxels showed reliable differences in the ACC ROI. Furthermore, vPFC and ACC activations were directly contrasted in an ROI (average activity in vPFC and ACC) -by-Condition (*go* vs. *nogo*) ANOVA, which revealed a marginally reliable ROI-by-Condition interaction: $F_{1,28} = 4.19$, $p = 0.05$. Finally, to examine differences in prefrontal and fronto-cingulate connectivity (see Pizzagalli *et al*., 2003), correlations (Pearson's *r*) were computed between the average activity in the ROIs and these correlations compared (Meng *et al*., 1992). All three correlations were significant vPFC–dPFC ($r_{30} = 0.87$, $P < 0.001$), ACC–vPFC ($r_{30} = 0.63$, $P < 0.001$), ACC–dLPFC ($r_{30} = 0.57$, $P < 0.01$). However, the correlation between the two right prefrontal ROIs was reliably higher than both ACC–vPFC ($Z = 2.56$, $P < 0.05$) and ACC– dLPFC ($Z = 3.17$, $P < 0.01$) correlations, whereas the latter two did not differ reliably ($Z = -0.77$, ns).

Discussion

The motivation of our go–nogo study was twofold. One facet of this study was the attempt to establish whether matching the frequency of

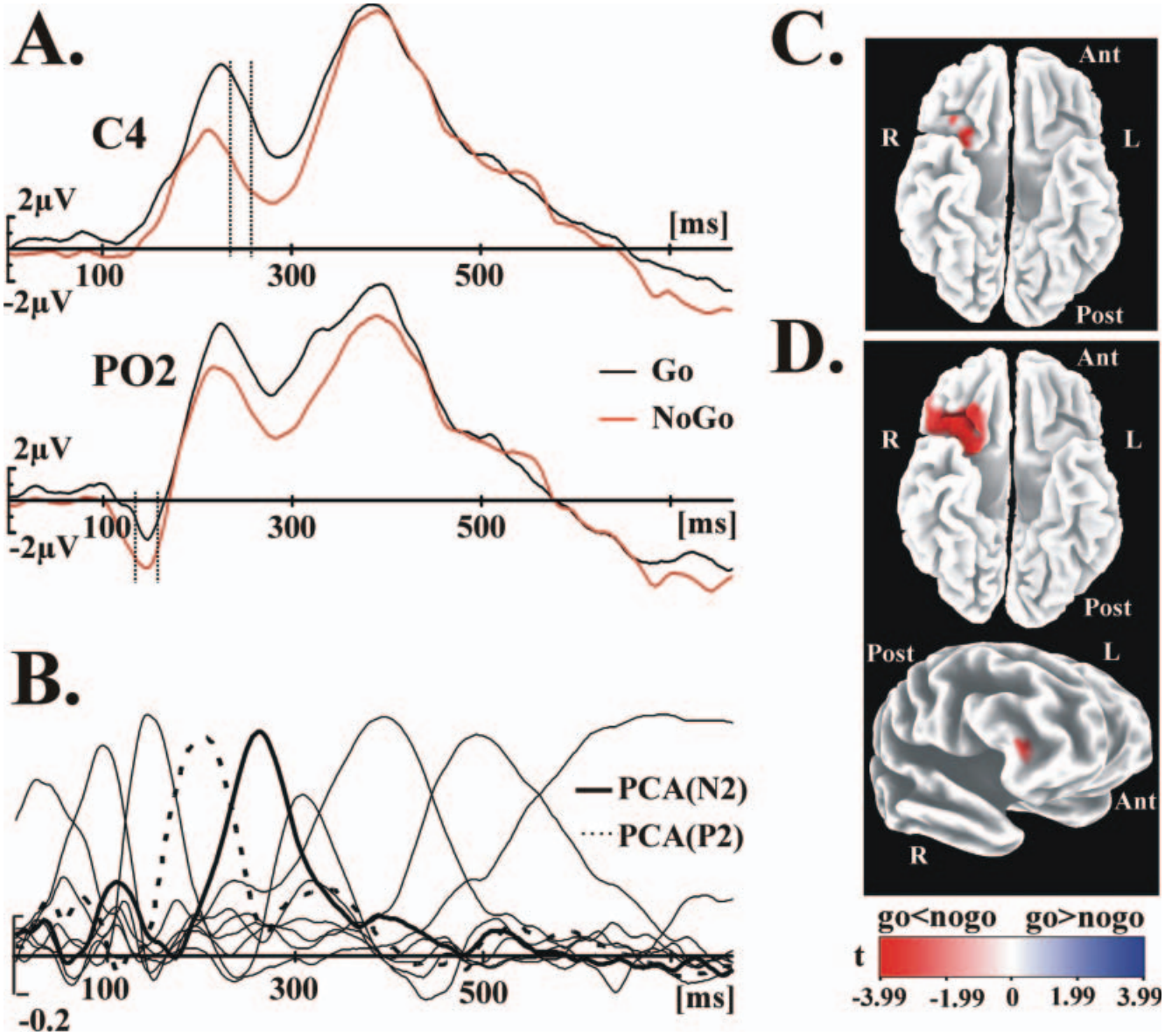

FIG. 1. (A) The ERPs *go* and *nogo* events at two representative scalp electrodes (one central and one posterior). Dotted lines represent the time-windows in which TANOVA found reliable differences between conditions. (B) Raw factor loadings for the nine temporal PCA components that explained over 95% of the variance. The two PCA components on which statistical analyses were performed are represented with dotted and bold lines. (C) Bottom view of the MNI brain with LORETA *t*-tests on the whole solution space. As in ROI *t*-tests (part D of figure, below), only surplus activity for the *nogo* condition relative to the *go* condition was found. (D) LORETA ROI *t*-tests. Top: bottom view of the vPFC ROI (minimum $t = -3.99$, x, y, z (MNI) = 25, 24, −20; Brodmann's area (47). Bottom: view from the right of the dLPFC ROI, represented on inflated cortical surface (minimum $t = -2.90$, x, y, z (MNI) = 46, 38, 8; Brodmann's area (46).

the go and nogo events had an impact on the previously described set of ERP go–nogo differences. Analysis across the whole ERP segment was performed by means of a data-driven procedure that simultaneously contrasted all scalp channels (the scalp vector) of the two conditions at each time-point (TANOVA). Of the two ranges of time-points in which the scalp vectors of the two conditions were reliably different, one corresponded to the N2 ERP component (see Fig. 1A). Conventional ERP amplitude analyses (ANOVA, *t*-tests) also found reliable effects in this time-window, especially in the frontal and parietal regions, bilaterally. Furthermore, the N2 effect does not seem to originate from an earlier difference in the P2 ERP component (or, indeed, the subsequent P3): reliable differences between conditions were found for the PCA component temporally corresponding to N2, whereas no effects were found in the PCA component corresponding to P2 (see Fig. 1B).

In contrast to the large N2 differences, no reliable TANOVA effects were found at latencies following N2, in particular in the P3 range. While a negative result does imply a lack of difference and should be interpreted with caution, our results suggest that, when *go* and *nogo* events are matched for frequency, the N2 difference is the robust effect. We conclude therefore that the go–nogo P3 effect may be largely driven by differences in frequency, or 'relative novelty'. P3-type components, especially those with frontal distribution, are known to be sensitive to novelty (Yamaguchi & Knight, 1991). Importantly, in most go–nogo paradigms that reported P3 differences, *nogo* events were rare relative to *go* events.

The earlier time-window, in which TANOVA revealed differences between the scalp vectors of the *go* and *nogo* conditions, corresponds to the visual N1 peak of the ERP, with larger N1 amplitude in the nogo condition (see Fig. 1A). We believe this may reflect an early signal from visual analysis areas that triggers the later inhibitory process, reflected by N2. Filipović *et al*. (2000) also found an enhanced N1 to *nogo* stimuli relative to *go* stimuli. They proposed that the N1 difference may reflect the decision to withdraw attentional resources from the task on *nogo* trials. Because previous ERP work indicates that N1 indexes increased (Mangun & Hillyard, 1991), rather than decreased attention to the stimulus, further work will have to clarify the functional significance of N1 in this context.

The other facet of our study was the use of cortical localization to clarify the functional meaning of the go–nogo ERP effects, in particular the presently disputed N2. Recently, dipole-modelling of N2 to ACC, as well as its colocalization with the error-related negativity was used to substantiate the proposal that N2 reflects conflict monitoring, rather than inhibitory processes (Nieuwenhuis *et al*., 2003). This is consistent with neuroimaging evidence that emphasizes the role of ACC in computing the degree of conflict between representations (Braver *et al*., 2001). A similar function in nonhuman primates seems to be performed by some neurons in the supplementary eye-fields, whose response appears to be modulated by degree of coactivation of gaze-shifting (i.e. *go*) and gaze-holding (*nogo*) neurons (Stuphorn *et al*., 2000).

On the other hand, neurophysiological studies with nonhuman primates (Watanabe, 1986), as well as human and nonhuman primate imaging studies (Konishi *et al*., 1999; Morita *et al*., 2004), show that ventral and dorsolateral prefrontal areas are likely to be the ones that accomplish inhibition. An ERP-LORETA study identified ACC, as well as ventral frontal substrates of the N2 effect (Bokura *et al*., 2001). This raises the possibility that, in addition to the conflict-sensitive system residing in ACC, a second, inhibitory, system may contribute to the documented go–nogo N2 differences. To isolate the latter system, we based our N2 localization on brain responses to *go* and *nogo* events that are equally rare, thus attempting to equate the degree of response conflict, while ensuring that each response tendency was prepotent.

Consistent with the hypothesis that equating stimulus frequency would decrease the amount of conflict between the go and nogo conditions but still ensure prepotent responses, we found higher activation in the N2 time-widow in vPFC and dLPFC, not in ACC (see Fig. 1C and D). This result emerged particularly clearly from our ROI analyses, which revealed in the N2 time-window higher activation in vPFC than in ACC, as well as stronger connectivity between the two right prefrontal ROIs, relative to their connectivity to ACC. Hence, we conclude that N2 effects reported in the literature may have two cortical substrates: ACC and vPFC/dLPFC, the former monitoring the conflict between competing response tendencies, and the latter inhibiting the inappropriate response. The fact that, when *go* and *nogo* events are matched for frequency, the cortical system that accomplishes inhibition dominates, indicates that the two functional components of N2 (with the associated anatomical substrates) can be studied in relative isolation. This can be of considerable clinical interest, in particular in the context of investigations of inhibition.

Abbreviations

ACC, anterior cingulate cortex; dLPFC, dorso-lateral prefrontal cortex; ERP, event-related potential; LORETA, low-resolution electromagnetic tomography; TANOVA, topographic analysis of variance; ROI, region of interest; vPFC, ventral prefrontal cortex.

References

Bokura, H., Yamaguchi, S. & Kobayashi, S. (2001) Electrophysiological correlates for response inhibition in a Go/NoGo task. *Clin. Neurophysiol.*, **112**, 2224–2232.

Braver, T.S., Barch, D.M., Gray, J.R., Molfese, D.L. & Snyder, A. (2001) Anterior cingulate cortex and response conflict: Effects of frequency, inhibition and errors. *Cereb. Cortex*, **11**, 825–836.

Brett, M., Johnsrude, I.S. & Owen, A.M. (2002) The problem of functional localization in the human brain. *Nat. Rev. Neurosci.*, **3**, 243–249.

Donchin, E. & Heffley, E.F. (1978) Multivariate analysis of event-related potential data: a tutorial review. In Otto, D. (Ed.), *Multidisciplinary Perspectives in Event-Related Brain Potential Research*. Government Printing Office, Washington, DC, USA, pp. 555–572.

Eimer, M. (1993) Effects of attention and stimulus probability on ERPs in a Go/Nogo task. *Biol. Psychol.*, **35**, 123–138.

Falkenstein, M., Hoormann, J. & Hohnsbein, J. (1999) ERP components in Go/Nogo tasks and their relation to inhibition. *Acta Psychol.*, **101**, 267–291.

Filipović, S.R., Jahanshahi, M. & Rothwell, J.C. (2000) Cortical potentials related to the nogo decision. *Exp. Brain. Res.*, **132**, 411–415.

Jodo, E. & Kayama, Y. (1992) Relation of a negative ERP component to response inhibition in a Go/Nogo task. *Electroenceph. Clin. Neurophysiol.*, **82**, 477–482.

Konishi, S., Nakajima, K., Uchida, I., Kikyo, H., Kameyama, M. & Miyashita, Y. (1999) Common inhibitory mechanism in human inferior prefrontal cortex revealed by event-related functional MRI. *Brain*, **122**, 981–991.

Lancaster, J.L., Woldorff, M.G., Parsons, L.M., Liotti, M., Freitas, C.S., Rainey, L., Kochunov, P.V., Nickerson, D., Mikiten, S.A. & Fox, P.T. (2000) Automated Talairach atlas labels for functional brain mapping. *Hum. Brain Mapp.*, **10**, 120–131.

Mangun, G.R. & Hillyard, S.A. (1991) Modulations of sensory-evoked brain potentials indicate changes in perceptual processing during visual-spatial priming. *J. Exp. Psychol. Hum. Perc. Perf.*, **17**, 1057–1074.

Meng, X.L., Rosenthal, R. & Rubin, D.B. (1992) Comparing correlated correlation coefficients. *Psychol. Bull.*, **111**, 172–175.

Morita, M., Nakahara, K. & Hayashi, T. (2004) A rapid presentation event-related functional magnetic resonance imaging study of response inhibition in macaque monkeys. *Neurosc. Lett.*, **356**, 203–206.

Mulert, C., Jäger, L., Schmitt, R., Bussfeld, P., Pogarell, O., Möller, H.-J., Juckel, G. & Hegerl, U. (2004) Integration of fMRI and simultaneous EEG: towards a comprehensive understanding of localization and time-course of brain activity in target detection. *Neuroimage*, **22**, 83–94.

Nichols, T.E. & Holmes, A.P. (2002) Nonparametric permutation tests for functional neuroimaging: a primer with examples. *Hum. Brain Mapp.*, **15**, 1–25.

Nieuwenhuis, S., Yeung, N., Van den Wildenberg, W. & Ridderinkhof, K.R. (2003) Electrophysiological correlates of anterior cingulate function in a go/no-go task: Effects of response conflict and trial type frequency. *Cogn. Affect. Behav. Neurosci.*, **3**, 17–26.

Pallier, C., Dupoux, E. & Jeannin, X. (1997) EXPE: an expandable programming language for on-line psychological experiments. *Behav. Res. Meth. Instruments Computers*, **29**, 322–327.

Pascual-Marqui, R.D. (1999) Review of methods for solving the EEG inverse problem. *Int. J. Bioelectromagnet.*, **1**, 75–86.

Pascual-Marqui, R.D., Michel, C.M. & Lehmann, D. (1994) Low resolution electromagnetic tomography: a new method for localizing electrical activity in the brain. *Int. J. Psychophysiol.*, **18**, 49–65.

Pascual-Marqui, R.D., Michel, C.M. & Lehmann, D. (1995) Segmentation of brain electrical activity into microstates: model estimation and validation. *IEEE Transactions Biomed. Engineering*, **42**, 658–665.

Pfefferbaum, A., Ford, J.M., Weller, B.J. & Kopell, B.S. (1985) ERPs to response production and inhibition. *Electroenceph. Clin. Neurophysiol.*, **60**, 423–434.

Pizzagalli, D.A., Oakes, T.R. & Davidson, R.J. (2003) Coupling of theta activity and glucose metabolism in the human rostral anterior cingulate cortex: An EEG/PET study of normal and depressed subjects. *Psychophysiology*, **40**, 939–949.

Pizzagalli, D.A., Oakes, T.R., Fox, A.S., Chung, M.K., Larson, C.L., Abercrombie, H.C., Schaefer, S.M., Benca, R.M. & Davidson, R.J. (2004) Functional but not structural subgenual prefrontal cortex abnormalities in melancholia. *Mol. Psychiatry*, **9**, 393–405.

Roberts, L.E., Rau, H., Lutzenberger, W. & Birbaumer, N. (1994) Mapping P300 waves onto inhibition: Go/Nogo discrimination. *Electroenceph. Clin. Neurophysiol.*, 44–55.

Roche, R.A.P., Garavan, H., Foxe, J.J. & O'Mara, S.M. (in press) Individual differences discriminate event-related potentials but not performance during response inhibition. *Exp. Brain Res.*, in press.
Stuphorn, V., Taylor, T.L. & Schall, J.D. (2000) Performance monitoring by the supplementary eye field. *Nature*, **408**, 857–860.
Talairach, J. & Tournoux, P. (1988) *Co-Planar Stereotaxic Atlas of the Human Brain*. Thieme, Stuttgart.
Van Veen, V. & Carter, C. (2002) The timing of action-monitoring processes in the Anterior Cingulate cortex. *J. Cogn. Neurosc.*, **14**, 593–602.
Watanabe, M. (1986) Prefrontal unit activity during delayed conditional go/no-go discrimination in the monkey. I. Relation to the stimulus. *Brain Res.*, **382**, 1–14.
Yamaguchi, S. & Knight, R.T. (1991) P300 generation by novel somatosensory stimuli. *Electroenceph. Clin. Neurophysiol.*, **78**, 50–55.